STUDY ON ELECTRON CLOUD AT THE BEPC*

Q. Qin, Z.Y. Guo, J. Cao, H. Huang, L. Ma, J.Q. Wang, J. Xing, G. Xu, C. Zhang, Z. Zhao,
Institute of High Energy Physics, Beijing 100039, P.R. China,
K.C. Harkay,
Argonne National Laboratory, Argonne, IL 60439, USA,
H. Fukuma, E. Kikutani, M. Tejima,
High Energy Accelerator Organization, 1-1 Oho, Tsukuba-shi, Ibaraki-ken, 305 Japan

1. Introduction

Since 1996, many experiments on photoelectron instability (PEI) have been carried out at the Beijing Electron Positron Collider (BEPC) in IHEP, China, in collaboration with KEK, Japan[1]. The studies obtained very productive results both in terms of experimental observations as well as analytical simulations, which agreed qualitatively with the observations at both BEPC and the KEKB factory.

Based on the detectors at the Advanced Photon Source (APS)[2,3] in ANL, USA, a specially constructed detector was installed in the BEPC storage ring in 2000. With this detector, it is hoped to measure the characteristics of the electron cloud and its dependence on beam parameters as well as the photoelectron (PE) and secondary electron (SE) yields and the energy spectrum of the electron cloud.

In this paper, the experimental results using the PE detector at the BEPC are presented. Some simulations related with the experiments are compared with the observation. At last, discussions are followed.

2. Instrumentations

A PE detector was made and installed on the BEPC storage ring. It has three layers with the same diameter of 80 mm and two mesh grids in front of the detector. The outermost grid is grounded, and a bias voltage is applied to the shielded grid. The collector is graphite-coated to lower the SE yield and is biased with a DC voltage of ~+48 V with batteries. The whole detector was mounted on an idle profile slot whose diameter is 100 mm located on the top of the vacuum chamber.

The PE detector is located in the third quadrant of the BEPC storage ring. Figure 1 shows the adjacent elements near the detector.

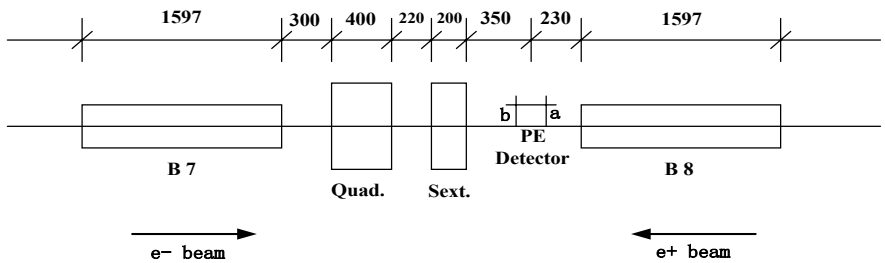

Figure 1. Position of the PE detector in the third quadrant of BEPC storage ring (in units of mm). (Seen from inside of the storage ring)

* Work supported by the Chinese National Foundation of Natural Sciences, contracts 19875063-A050501 and 19975056-A050501.

Being so close to the dipole, B8, the PE detector has to be shielded from the magnetic field with the layers of high and low permeability "mu-metal" sheets and nickel alloy sheets. After being shielded, the fields at the points "a" and "b" in Fig. 1, the rightmost and leftmost points of the detector, are only 9 Gauss and 0, respectively. At the center inside the detector chamber, the fringe field of the dipole is measured using a model chamber installed in a reference dipole, which as the same field of the dipoles in the storage ring. The result confirms the effect of shielding.

When the beam passes the annular gap between the detector and the support barrel, the induced wake field will generate some higher order modes and cause a temperature rise. A temperature monitor was mounted on the center of the outer surface of the flange, which connects the detector and the supporter, to confirm the effect of this unshielded gap.

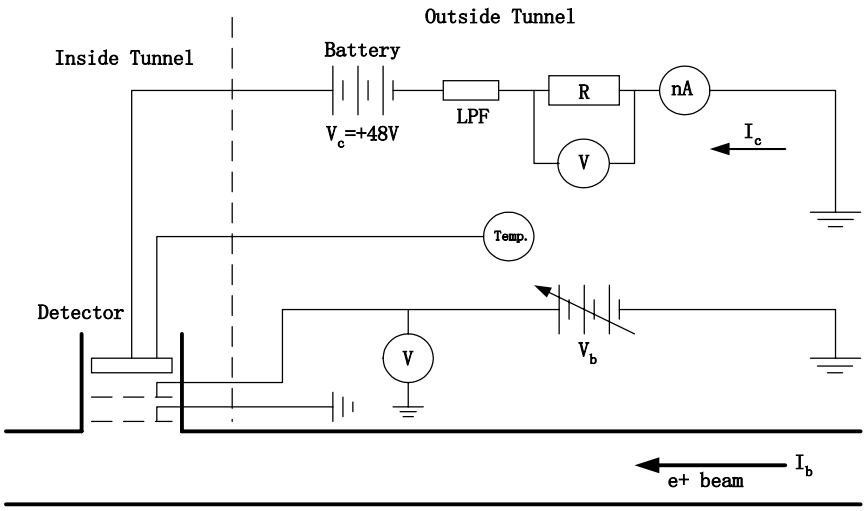

Figure 2. Setup of all apparatus in the experiment.

All the apparatus for observation of the PE are setup as shown in Fig. 2. The detector is first connected in series with the batteries. Then, a low pass filter (LPF) is used to make sure that the signal of the collector is from the electron only. After the LPF, a 0.1 MΩ resistor is connected to check the direction of the current from the collector with a voltmeter connected across the resistor. The current of PE is measured with the nanoammeter, which is connected between the resistor and ground. It crosschecks the readings of the voltmeter.

3. PE Measurement

3.1 Beam parameters

The BEPC can be operated as a collider with electron and positron beams, and a dedicated synchrotron radiation facility as well. Table 1 lists main parameters of the BEPC storage ring. Table 2 lists the beam parameters of the different optics applied in the experiment.

Table 1. Main parameters of the BEPC storage ring

Beam energy	1.3 GeV	Critical energy	0.471 keV
Circumference	240.4 m	Revolutionary frequency	1.247 MHz
Dipole field	0.419 T	Dipole length	1.597 m
Bending angle/dipole	0.1547 rad	Bending radius	10.336 m
RF frequency	199.535 MHz	Harmonic number	160
RF voltage	0.2 ~ 1 MV	Bucket length	5 ns
SR energy loss/turn	24.3 keV	Beam energy spread	3.46×10^{-4}

Table 2. Main beam parameters of the different optics used in the experiment

Beam parameter	165#	14#	89#
Emittance	0.3 mm·mrad	0.13 mm·mrad	0.028 mm·mrad
Momentum compaction	0.044	0.036	0.016
Betatron tunes	5.82/6.75	5.82/6.74	8.72/4.75
Natural chromaticity	-10.68/-17.04	-8.18/-10.08	-13.10/-7.53
Chromaticity with sextupole	6.00/6.00	4.00/4.00	1.5/1.5
β_x/β_y at PE detector	12.05/5.15 m	6.62/5.45 m	6.27/7.19 m
η_x at PE detector	2.22 m	1.63 m	0.67 m
H/V coupling	~5%	~5%	~5%

The beam orbits also depend on different optics. In the experiment, only one RF cavity is used with an RF voltage of ~220 kV. The bunch length is about 4 cm.

3.2 Instrumentation check with beam

As we mentioned before, the LPF filters the beam-induced RF noises. The detector current (I_c) is measured as a function of beam current for LPFs with different cutoff frequencies, shown as Fig. 3. Then, in the PE experiments, a 150 MHz LPF is applied.

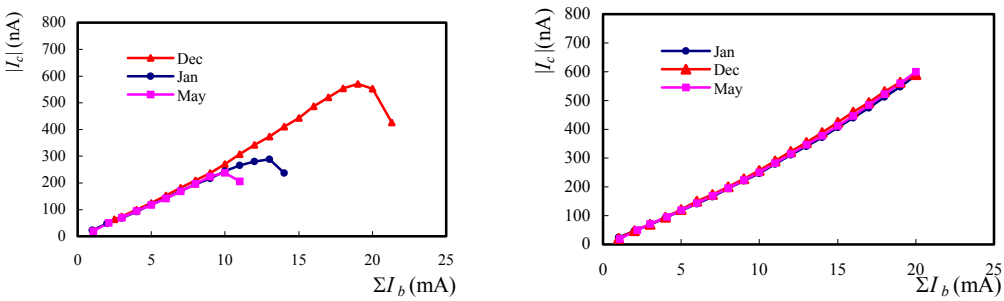

Figure 3. Effect of LPF. (Left: without LPF, Right: with a 150 MHz LPF)

During the experiment, the temperature monitor displays 24±1°C with no change, which shows the HOMs effect due to the annular gap between the detector and its support barrel is minimal. All these confirm the validity of the whole measurement system.

The bias voltage is fixed at +40 V for maximum signal after a voltage scan was made, shown as Fig. 4.

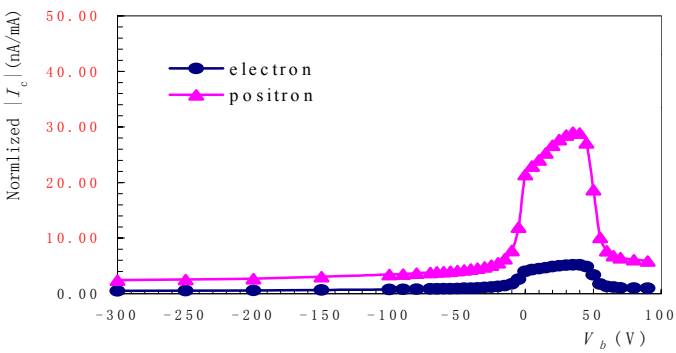

Figure 4. Detector current when bias voltage is scanned.

From Fig. 4, we can see that the PE signal created by the electron beam is 6 times lower than that created by the positron beam. One possible reason is that the detector is located 6 times closer to the downstream dipole (B8) for the positron than the distance from the detector to the downstream dipole (B7) for the electron beam, as Fig. 1 shows. Another reason maybe comes

from the interaction of the PE and positron beam may cause more electrons to be deflected into the detector. In the following experiments, positron beam is used.

3.3 Dependence on beam current

In the experiment, we measured the collected electron current I_c as a function of beam current I_b in the cases of single and multi-bunch. Normalized by I_b, I_c varies linearly with the I_b, similar to curve in the right plot of Fig. 3. The slope is about 25nA/mA at the bunch current of 2 mA. Fig. 5 shows that there is no significant difference between the single and multi-bunch cases. In the multi-bunch case, the bunch current is approximately 2mA.

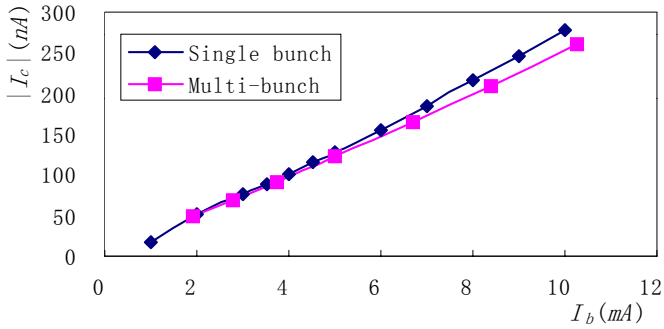

Figure 5. Comparison of single and multi-bunch cases.

A saturation effect, in which electron generation and loss equilibrate, was found in the APS's experiment. We did the same on the BEPC with a long bunch train and a weak bunch current, even 40 bunches are used with the bunch current of 1 or 2 mA (I_b is 40 or 80 mA), but did not find the very clear saturation effect, shown as Fig. 6. The reason might be the fact that the detector is located very near the dipole and there is no antechamber, causing the primary photoelectron emission to dominate over secondary electron emission.

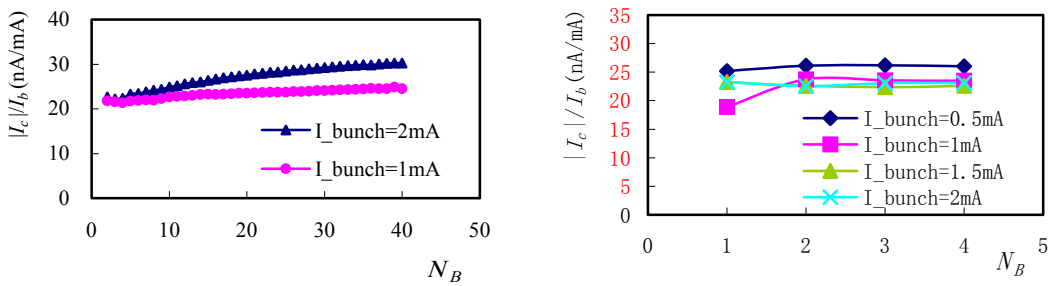

Figure 6. Effect of bunch train length. (Left, $S_b = 2$ buckets. Right, $S_b = 5$ buckets)

The derivative of the normalized I_c-V_b curve gives the photoelectron energy distribution, shown as Fig. 7.

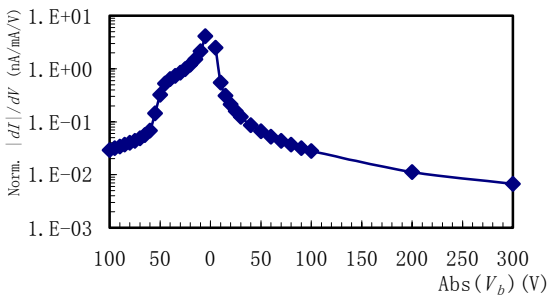

Figure 7. Photoelectron energy distribution.

3.4 Secondary electron (SE) measurement

The energy gain of the electrons kicked by the beam is determined by $\Delta p = 2m_e N_b r_e c/a$, where a is the radial distance from the beam and r_e is the classical electron radius. From the APS, on which the beam-induced multipacting (BIM) was observed with 20 ns bunch spacing (7 buckets) and ~1.5 mA/bunch (vertical chamber height 42 mm), we can estimate that the BIM may be expected at the BEPC with ~30 ns spacing (5~6 buckets) and ~6 mA/bunch (vertical chamber height 58 mm). But in our measurements, such a dramatic amplification of the signal due to the SE is not observed when the bunch spacing and current are scanned from 1 mA/bunch to 6 mA/bunch with the bunch spacing from 1 to 12 buckets in a bunch train of 5 and 10 bunches, shown in Fig. 8.

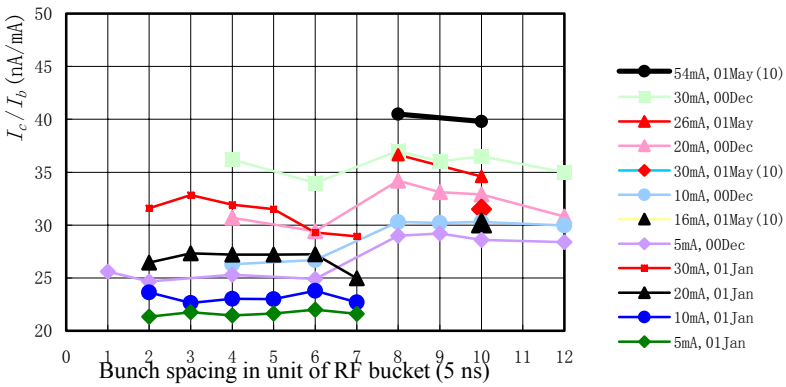

Figure 8. Normalized electron current as a function of bunch spacing and current.
(The legend gives the beam current.)

From Fig. 8, we can see the normalized electron current increases when the bunch current increases. The reason may come from the short distance between the bending magnet and the detector, which may cause the photoelectrons to dominate and possibly suppress the SE.

3.5 Dependence on beam parameters

1) Closed orbit

The collector current I_c as a function of beam current was measured with the different closed orbit. The PE distribution is found to be quite sensitive to the beam position, since the I_c has 1 nA linear increment when the vertical closed orbit increases 1mm with an I_b of 1mA, shown as Fig. 9.

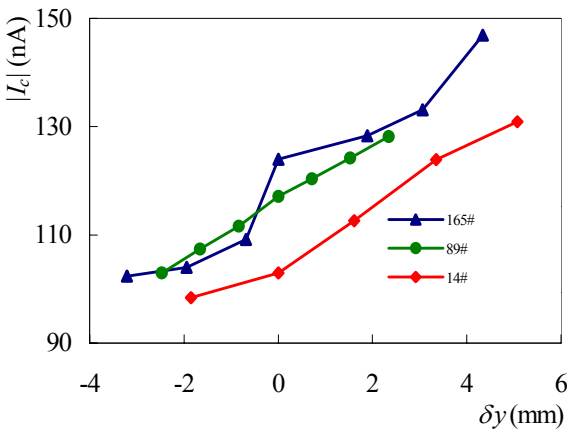

Figure 9. Correlations between vertical closed orbit and I_c for different beam optics.

2) Beam energy and emittance

The beam energy and emittance are not sensitive to the collector current, I_c, when the closed orbits are fixed. Fig. 10 shows the correlations between beam energy and normalized I_c for different optics, which have different emittances.

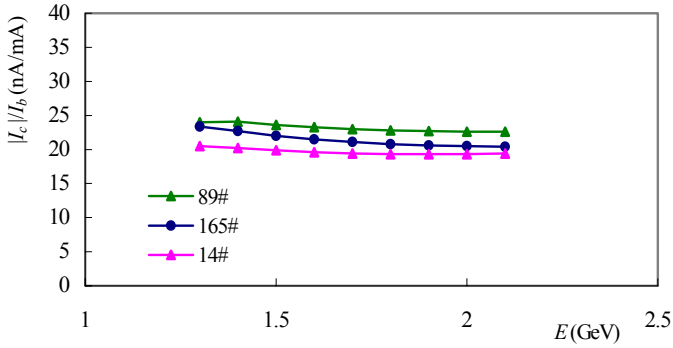

Figure 10. Normalized I_c varies with beam energy in different optics.

3) Chromaticity

Scans of bias voltage were done for different chromaticity, shown in Fig. 11. No any clear differences were found.

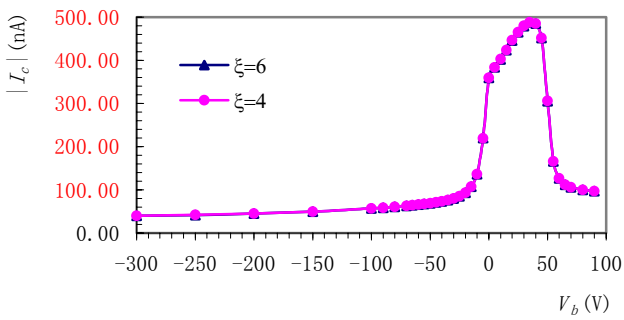

Figure 11. Bias voltage scan for different chromaticities.

4) Stable and unstable beams

In the BEPC storage ring, a kind of vertical coupled-bunch instability happens and a broad spectrum appears for the positron beam when the threshold beam current of 9.7 mA is reached. We set the beam conditions as the total beam current of 9.8 mA with 160 bunches uniformly distributed around the storage ring in each bucket, the beam instability occurs as before. The I_c is then measured in the cases of stable and unstable beams. The relations of I_c vs. I_b for both stable and unstable beams are shown in Fig. 12.

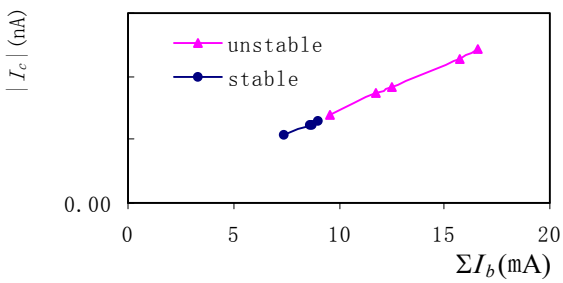

Figure 12. I_c vs. ΣI_b for stable and unstable beams.

The instability is also observed with 16.6 mA in 116 bunches, and the I_c dependence is the same as the stable case. This indicates the beam oscillation due to PEI does not influence the yield of the photoelectron.

3.6 Solenoid effect

Solenoid coil, winding downstream the dipoles, is a possible way to cure the PEI, like KEKB LER. In BEPC storage ring, we installed a pair of coils, with each coil winding on each side of the detector, to observe the influence of the solenoid field. The currents of the coils, I_s, are ±20A, which can generate several tens of Gauss magnetic field. Fig. 13 shows the I_c vs. I_b when solenoid has different currents. When we scan the bias voltage V_b, I_c is given in Fig. 14.

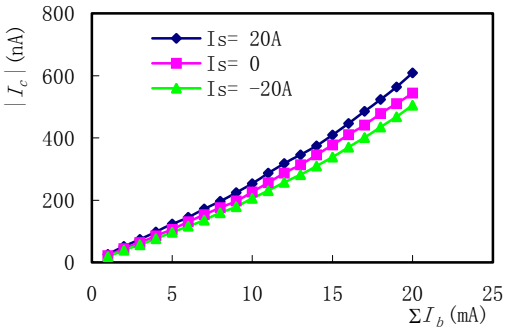

Figure 13. I_c changes with I_b for different I_s.

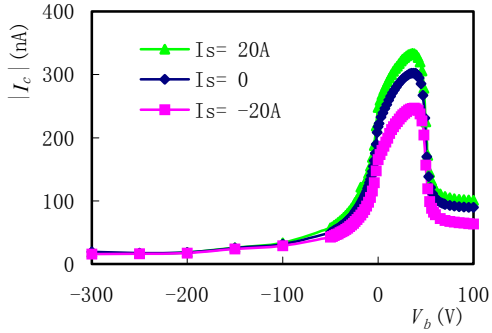

Figure 14. Bias voltage scan for different I_s.

It can be seen that the solenoid field does influence the electron cloud at the location of the PE detector, but it is not a strong effect. The difference when the direction of the solenoid field changes comes from the combining effect of the solenoid field and the fringe field of the dipole, which locates near the detector. The combined field was also measured in the same way as the fringe field measurement described previously.

4. Simulations

Some preliminary simulations on the PE generation was done with the code developed by Y. Luo[4]. First, the transverse distribution of the PE in the BEPC vacuum chamber is simulated with different reflectivity, shown in Fig. 15. In the simulation, an effective radius of the aluminum vacuum chamber in the BEPC storage ring is assumed as r = 50 mm.

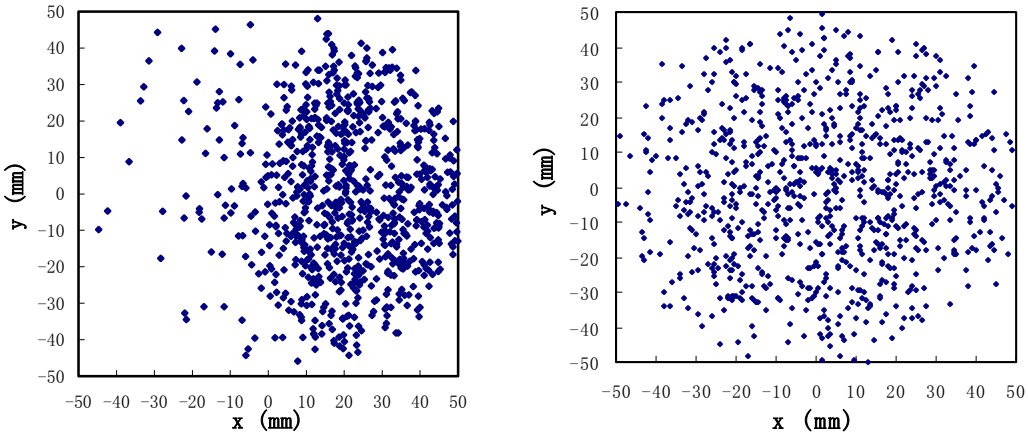

Figure 15. Transverse distribution of the PE. (Left: Reflectivity=0.1, Right: Reflectivity=0.9)

For a real machine, a reflectivity of 0.98 is chosen in the simulation. The energy distribution of the

PE is selected as 5eV±5eV, and the yield of PE is Y'=0.1. The emission yield of the SE is given as the formula of

$$\delta(E,\theta)=\delta_{\max}\cdot 1.11\cdot\left(\frac{E}{E_{\max}}\right)^{-0.35}\cdot\left(1-\exp\left[-23\cdot\left(\frac{E}{E_{\max}}\right)^{1.35}\right]\right)/\cos\theta$$

with a $\cos\theta$ distribution as the angle distribution. The yield of SE is chosen as δ_{max}=1.5, and the E_{max} in the above formula is E_{max} = 250 eV. The energy distribution of SE is 0eV±5eV, with the angle distribution of $\cos\theta$ distribution. Fig. 16 gives the simulation results on the PE creation.

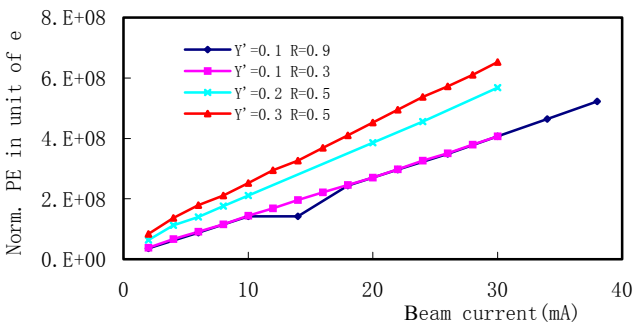

Figure 16. PE creation in different yields and reflectivity.

We also simulate the PE dependence on beam energy and the bunch spacing, shown in Fig. 17 and 18.

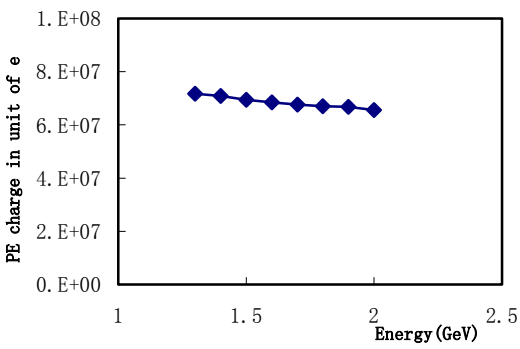

Figure 17. PE current as a function of beam energy. (Single bunch, I_b = 2 mA)

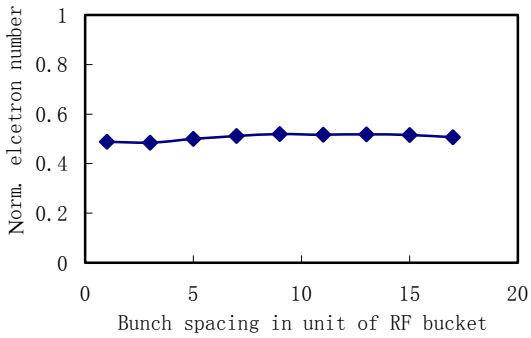

Figure 18. PE current as a function of bunch spacing. (S_b = 5 ns, n_b = 5, I_b = 5 mA)

5. Discussions

5.1 PE measurement

Detailed measurements of the properties of PE cloud were carried out at the BEPC storage ring under various machine conditions for both stable and unstable beams. Comparisons were made between single and multi-bunch cases as well as for positron and electron beams. I_c varies linearly with the beam current I_b as expected, since the photoelectron number is proportional to the photon intensity and the beam current. This is the same behavior for single bunch and a number of multi-bunch patterns. No saturation process is observed up to 40 bunches with 1 or 2 mA/bunch. We observed very weak dependence on bunch spacing, using 5 and 10 bunches with 1 to 6 mA/bunch up to the 12-bucket spacing. No beam-induced multipacting was observed at the BEPC yet. No significant differences were observed in I_c behaviors for stable and unstable beams.

5.2 Simulations

Primary simulations give some consistent results with the experiments, especially the multipacting condition and the dependences of beam parameters. More simulation studies are still under way.

5.3 Further studies

The distance between detector and dipole influences the measurement of SE and the saturation process very much. Two new detectors, modified as encircling the grounded grid but isolated from the retarding grid and the collector to avoid the I_c electrical leak from HOMs excited through the gap between the detector and the port, will be installed soon in the places far from dipoles. One will be installed on the vertical port, similar as the present one, and another will be installed on the horizontal port. The time structure of I_c signal and the machine parameter dependences would be studied furthermore. Better shielding is necessary on the existing detector to avoid the fringe field of the dipole.

6. Acknowledgements

The authors are grateful to the effective work of the BEPC operation team during the experiment. We would also like to thank Dr. R. Rosenberg from ANL, for his suggestion on shielding the detector, and Dr. Y. Luo, for his code of simulation.

References

[1] Z.Y. Guo, et al, Proc. of PAC'97, 1997, EPAC'98, APAC'98, 1998.
[2] K. Harkay and R. Rosenberg, Proc. of PAC'99, 1999.
[3] R. Rosenberg, K. Harkay, NIM A 453 (2000) 507.
[4] Y. Luo, IHEP Ph. D dissertation, 2000.